STRONG-MOTION DATA FROM THE M6.0 PARKFIELD EARTHQUAKE OF SEPTEMBER 28, 2004

Anthony Shakal, Vladimir Graizer, Moh Huang,
Hamid Haddadi and Kuo-wan Lin

California Strong Motion Instrumentation Program
California Geological Survey, Sacramento, CA

Abstract

The M6.0 Parkfield earthquake of September 28, 2004 that occurred on the San Andreas fault near the town of Parkfield in central California produced the most extensive and dense set of near-fault strong motion recordings ever obtained in California. As a result of a widely accepted likelihood of an earthquake in the area, a large number of strong motion stations had been deployed in the area. The arrays and the resultant strong-motion measurements of the earthquake, as well as preliminary observations are described here. The data includes very high variability in the near fault motion and accelerations as high as 2.5g.

Introduction

The Parkfield earthquake occurred along the same segment of the San Andreas fault that ruptured during the 1966 Parkfield earthquake, resulting in a unique set of strong motion measurements by arrays specifically designed to record an event on this fault segment. The data and arrays are described more comprehensively in Shakal et al. (2005), and more general seismological results are described in Langbein et al. (2005).

A total of 56 three-component strong-motion recordings of acceleration were obtained within 20 km of the fault, with 49 of these being within 10 km of the fault. The strong motion measurements in the near fault region are highly varied, with significant variations occurring over relatively short distances. A map of near fault peak acceleration (Figure 1) shows striking variations over only a few km. The map also shows concentrations of strong shaking at both ends of the fault.

Peak accelerations in the near fault region range from 0.13 g to over 2.5 g (perhaps the highest acceleration recorded to date). The largest acceleration occurred near the northwest end of the inferred rupture zone, consistent with a model in which the strongest asperities on the fault occurred along this segment of the fault. These motions are consistent with directivity due to a fault rupturing from the hypocenter near Gold Hill to the northwest. However, accelerations up to 0.8g were also observed at the south end of the Cholame Valley near Hwy 46. These values are consistent with bilateral rupture to the southeast of the hypocenter, as included in the source modeling of Liu et al. (2005). The town of Parkfield itself had relatively low ground acceleration, only a fraction of that at stations within 2 km. However, the ground displacement at Parkfield was not small, dominated by periods between 0.6 and 1 second.

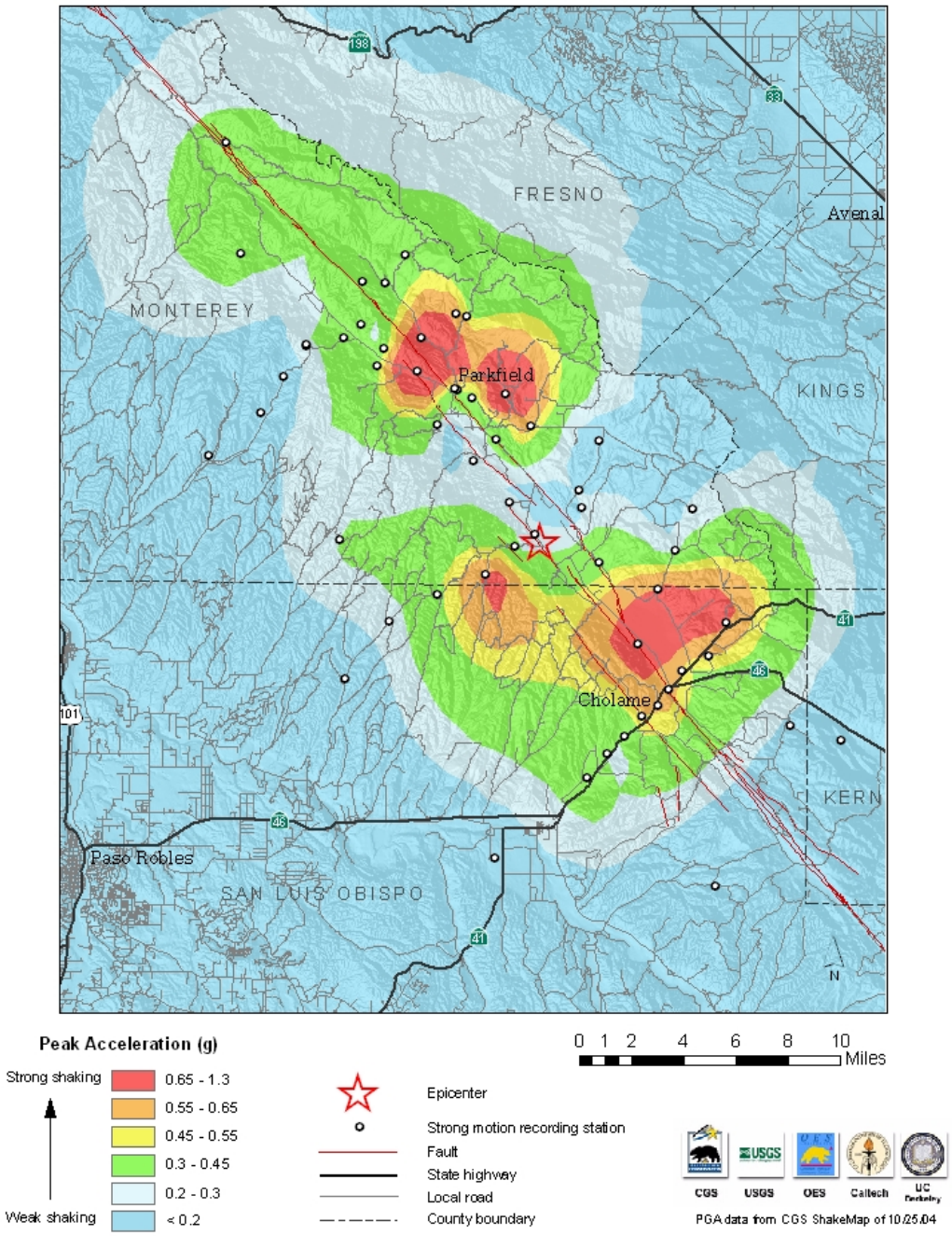

Figure 1. Contour map of near-fault peak ground accelerations. Locations of stations (CGS and USGS) are indicated. Areas of high amplitude shaking at the northwest and southeast end are clear, with low accelerations in the central segment near the epicenter (star).

The Parkfield Strong Motion Array

The Parkfield strong motion array was designed to measure ground shaking close to a fault. Shown in Figure 2, the array includes instruments installed and maintained by both the California Geological Survey (CGS) and the U.S. Geological Survey (USGS). The CGS Parkfield strong motion array (McJunkin and Shakal, 1983) was installed during the early 1980s and consists of a network of 45 primarily analog strong motion recorders. Shortly after installation the array recorded an important set of records during the 6.5 M_L 1983 Coalinga earthquake (Shakal and McJunkin, 1983). This data is important for comparison with the new data from the same stations to help understand site effects. The largest acceleration from that earthquake, which occurred 35 km north of the array, was 0.28g at Fault Zone 14; the rest of the stations had accelerations in the .05 - .20g range.

Complementing the initial set of recorders, after the Parkfield earthquake prediction experiment was initiated (Bakun and McEvilly, 1984) a network of 12 high-resolution GEOS recorders designed to provide on-scale broad-band measurements of earthquake shaking was installed by the USGS (Borcherdt et al., 1985; Borcherdt and Johnson, 1988). The GEOS stations include short period high-resolution measurements from collocated accelerometers and velocity transducers that provide a recording range extending from seismic background noise levels to 2g in acceleration. In addition, several sites include collocated volumetric strain sensors. The GEOS instruments obtained strong motion records at 11 sites. The values they recorded are very similar to values obtained from nearby classic strong motion recorders. The 180 dB dynamic resolution of the recordings will allow much more detailed analysis than analog film instruments, or digital instruments with less resolution.

Volumetric strain recordings (Borcherdt et al., 2004) were obtained at four of the GEOS sites and are among the first such recordings obtained in the near source region of an earthquake this large. They extend the bandwidth and dynamic range for near source motions to periods longer than possible from accelerometer measurements alone.

Geologic Setting

Parkfield is at the northwestern end of the Cholame Valley, which extends from the vicinity of Parkfield to the southeast, where Hwy 46 crosses the valley (Figure 2). The valley lies between the Cholame Hills to the west and the southern Diablo Range to the east. The San Andreas Fault forms the boundary between the Salinian block on the west and the southern Diablo Range on the east. The geologic structure is complex to the east of the fault, where mostly metamorphic sedimentary and metamorphic rocks are exposed. The geologic structure is less complex to the west, with sedimentary deposits of late Cenozoic age over more complex Mesozoic bedrock of the Salinian block (Dickinsen, 1966; Dibblee, 1973; Jennings, 1977; McJunkin and Shakal, 1983).

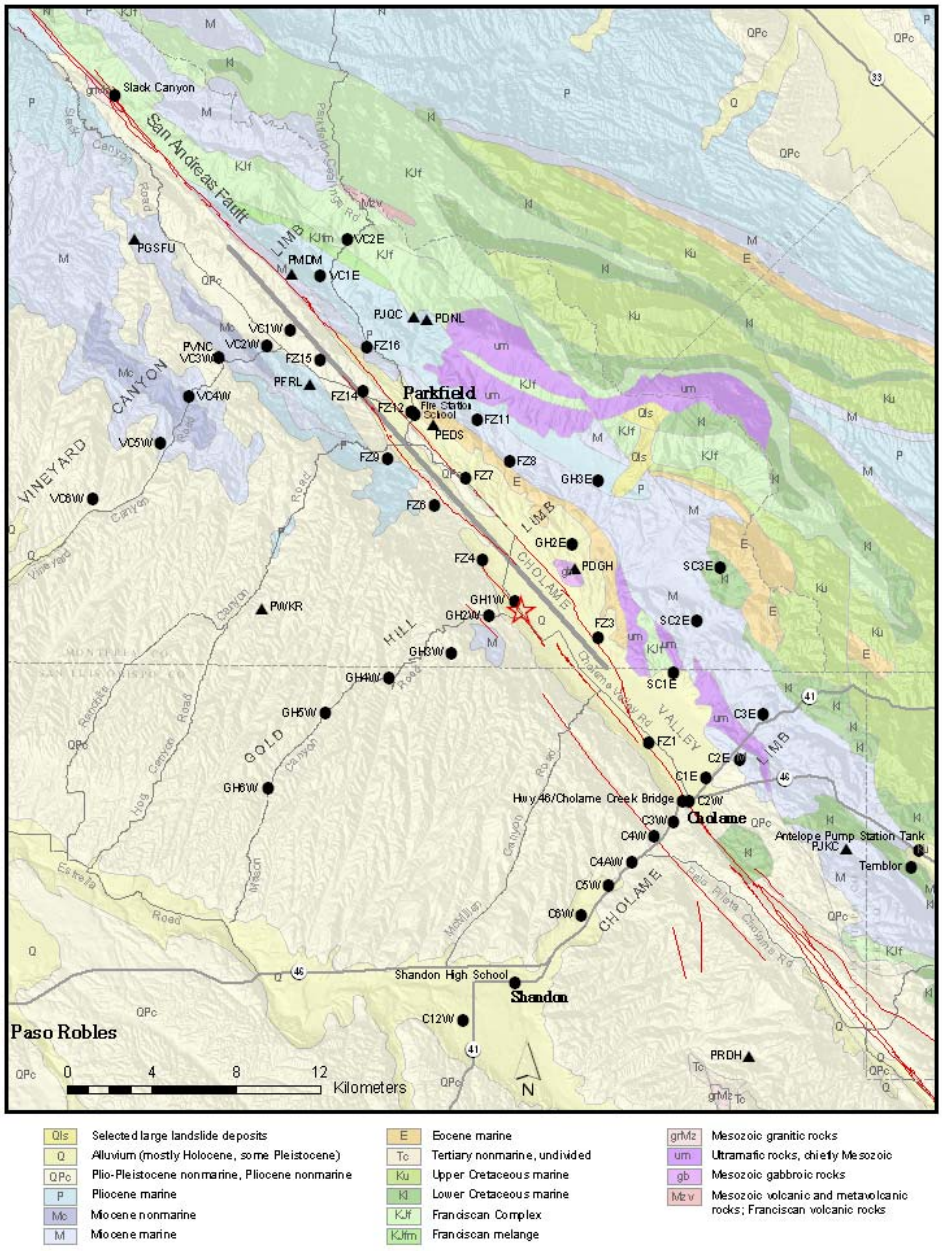

Figure 2. Stations in the Parkfield array plotted on a map of the regional geology (Jennings, 1977). Circles are CGS (mostly analog) strong motion stations; triangles are USGS high-resolution GEOS stations. The main strands of the San Andreas Fault and the earthquake epicenter (star) are shown. East of the alluvial Cholame Valley the geology of the Diablo Range is highly complex. The geologic structure is less complex to the west, with late Cenozoic sedimentary deposits. The earthquake surface faulting extends from near the epicenter northwest to Middle Mountain, northwest of Parkfield (Langbein et al., 2005). The line source model of Dreger (2004) is shown for reference. Codes for the CGS stations reflect the naming system (VC for Vineyard Canyon stations, GH for Gold Hill, C for Cholame, SC for Stone Corral, and FZ for Fault Zone).

Array Configuration

The Parkfield strong motion array was designed to meet several measurement objectives. A major goal was to provide near-fault ground motion data complete enough that details of the rupture propagation process could be resolved. The configuration of the array, shown in Figure 2, reflects compromises between idealized objectives and practical aspects of logistics, field access, and site conditions. The array has the shape of a backward 'E', with three branches extending to the west, and a central near-fault pattern of stations paralleling the fault (called fault zone stations).

The three alignments, or limbs, of stations extending to the southwest, perpendicular to the fault, are called the Cholame, Gold Hill and Vineyard Canyon limbs. They allow study of attenuation with distance at near-fault distances. They extend to the west because the underlying formation is more uniform than the geologic structure to the east. The topography of the Diablo Range to the east also makes access more difficult; a general goal was to site the array stations to be accessible from normally passable roads.

The stations of the three limbs are sequentially numbered outward from the fault for each limb, starting from 1W for stations to the west, and 1E for stations to the east. The central set of stations are called the Fault Zone stations, and are sequentially numbered from Fault Zone 1 on the south end, near Hwy 46, to Fault Zone 16, north of Parkfield.

Several of the CGS stations in the Cholame limb along Highway 46 correspond to stations of the original 1966 array (Cloud and Perez, 1967). As installed in 1982, the array shared 4 locations with the 1966 set (Cholame 2WA, 5W, 8W and 12W). The reality of property owner issues compromised this set since, however. Station 8W was removed at the property owner's request, and 5W was moved about 1 km to the west. The location of 2WA approximately corresponds to the location of the Station 2 site of 1966. Only 12W is at the same location as the 1966 station.

The CGS stations are augmented by 12 high-resolution GEOS stations interspersed in the above pattern, installed by the USGS, with accelerometers and velocity transducers, and four have borehole volumetric strain dilatometers (Borcherdt et al., 2004). These sensors yielded some of the first measurements of strain during strong earthquake shaking.

Peak Acceleration vs Distance

A comparison of the peak accelerations for this event with those predicted by standard relationships is useful. A plot of peak acceleration versus distance to the fault for the available set of 92 records is shown in Figure 3. The distances range from less than 0.5 km to 170 km from the fault. An important feature that makes this data set very important is the large number of recordings obtained within 10 km of the fault zone, which provide a rare opportunity for testing hypotheses about near-fault ground motion.

Five attenuation relationships for a strike slip fault are shown in Figure 3, including Boore-Joyner-Fumal (BJF97, Boore et al. 1997), Sadigh et al. (1997), Abrahamson and Silva (1997), Idriss (1993) and Campbell (1997). (For BJF97 an average shallow Vs of 350 m/sec was used, and the Sadigh et al. and Campbell relationships for soft soil sites were used, as most of the array sites are on alluvium). These attenuation relationships were developed for distances less than 100 km. Recordings from modern digital instruments provide data that is precise to low shaking levels. The data for this event, and other recently recorded earthquakes (e.g., M7.3 Hector Mine and M6.5 San Simeon; Graizer and Shakal, 2005) provide information needed to extend the existing attenuation relationships beyond previous limitations (80-100 km) out to distances of 200 km, important for larger earthquakes.

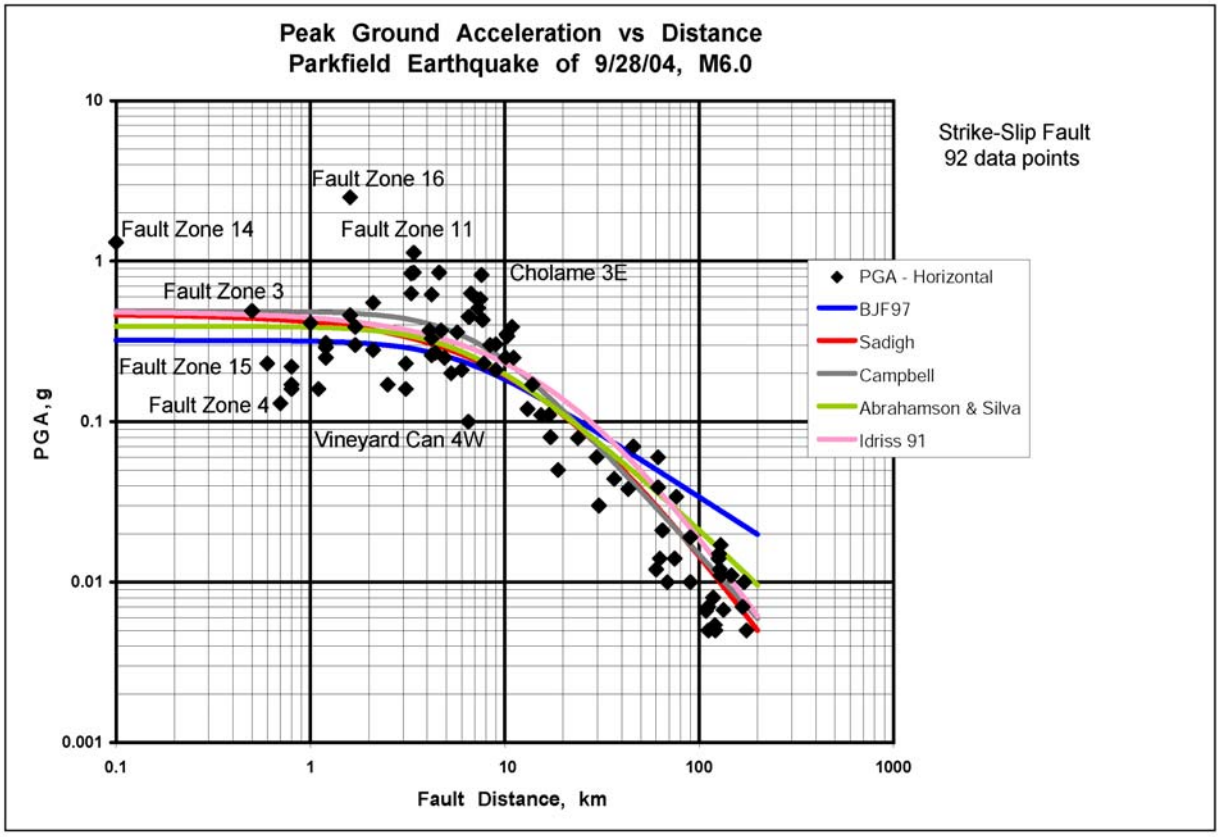

Figure 3. Horizontal uncorrected peak ground acceleration versus distance to the fault for data from the Parkfield earthquake of September 28, 2004. The attenuation relationship of Boore, Joyner and Fumal (1997; BJF97) is shown as well as the relationships of Sadigh et al. (1997), Campbell (1997), Abrahamson and Silva (1997) and Idriss (1993). The peak ground acceleration observations drop off more rapidly with distance than most of the curves. The largest peak accelerations are plotted here though strictly some (Sadigh, Campbell, Idriss) use the geometric mean of the two horizontals (which typically reduces the plotted value by 10%). All five relationships are extrapolated beyond 80 or 100 km. (Here and in subsequent plots the peak acceleration for Fault Zone 16, though known to be over 2.5g, is plotted at 2.5g.)

Directivity in Peak Acceleration and Velocity

To study the effect of unilateral rupture directivity on peak ground acceleration the data set was split into two groups: stations located in the forward direction from the epicenter and in the backward direction. This grouping is based on the preliminary source modeling of unilateral rupture propagating from the epicenter to the northwest. In the resulting plot (Figure 4), directivity effects are not apparent in the near fault acceleration data for distances less than 10 km from the fault. At greater distances some differences in forward and backward directivity stations are suggested. The PGA data in the forward direction appears to attenuate slightly more slowly than in the backward direction.

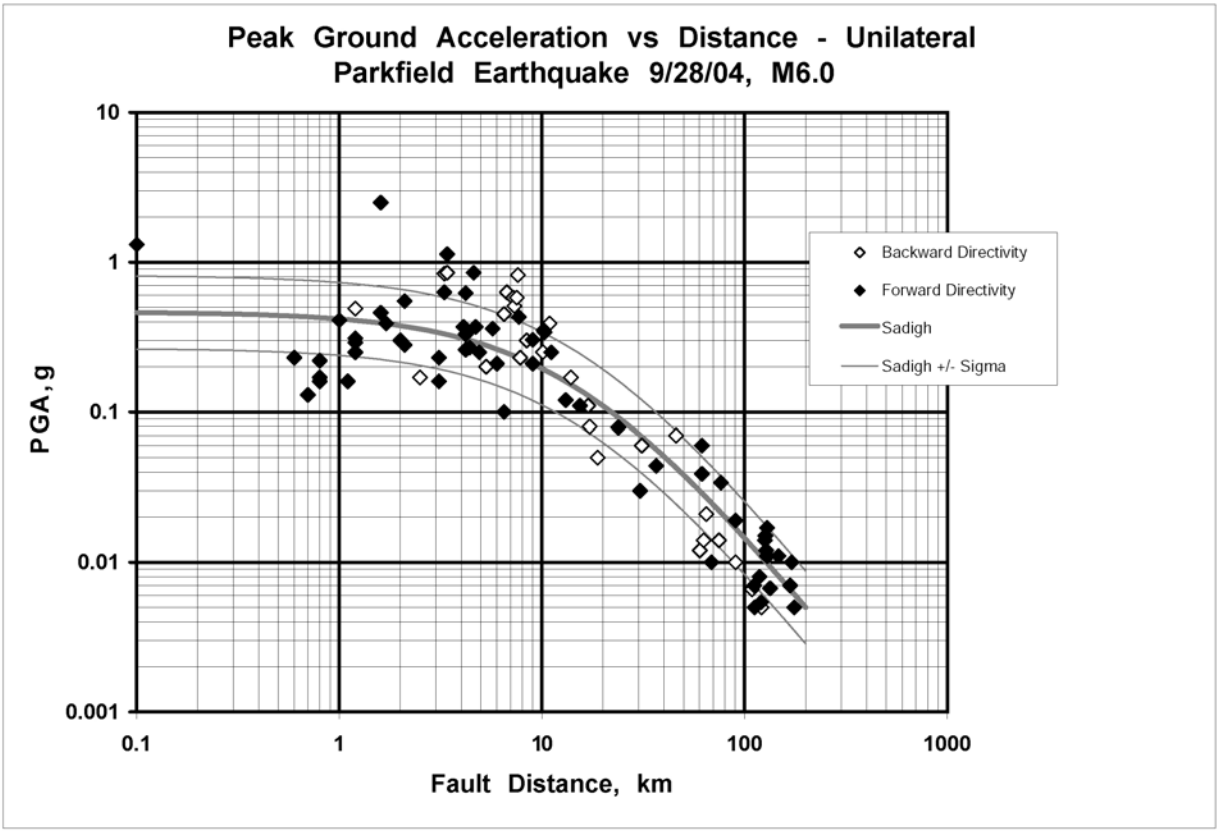

Figure 4. Peak ground acceleration considered as a function of simple directivity and unilateral rupture. The symbols are identified as either forward directivity or backward directivity according to the station locations either north or south of a northeast-southwest line passing through the epicenter, perpendicular to the fault. The Sadigh curve from Figure 3 is shown for reference. No difference is observable in the near-fault zone within 10 km of the fault.

The effect of bilateral rupture may be explored: some early modeling suggests bilateral rupture, with the southeast termination of the rupture located approximately 5 km southeast of the epicenter. In this model, the rupture starts at the hypocenter and propagates 5 km to the southeast and 20 km to the northwest. With this model in mind

the data were split into a group that were within ±45 degrees of the fault orientation, in either direction, and another group that were outside these regions. The resulting plot (Figure 5) shows more separation of the forward directivity stations than that shown in Figure 4. Figure 6 shows a similar plot of peak ground velocity, and the directivity effect is more apparent.

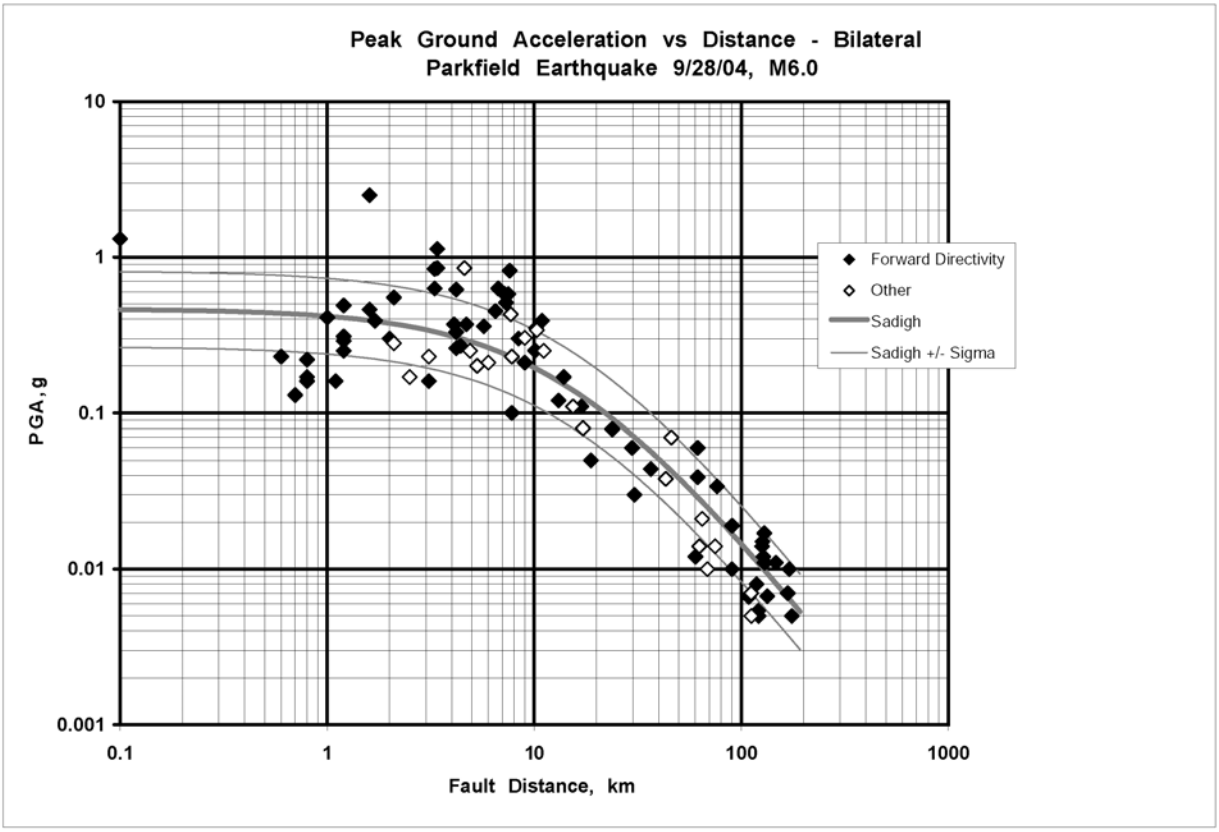

Figure 5. Peak acceleration versus distance data separated according to forward directivity in the case of bilateral rupture propagation, as described in the text. The Sadigh curve from Figure 3 is again shown for reference.

Near-Fault Ground Motions

The strong motions in the near fault region are highly varied, with significant variations over relatively short distances, as reflected in the map of Figure 1. The map also shows concentrations of strong shaking at both ends of the fault. Peak ground acceleration in the near-fault region ranges from 0.13 g at Fault Zone 4, to 1.31 g at Fault Zone 14, ten times larger, to over 2.5 g at Fault Zone 16 (where the motion exceeded the instrument capacity). The largest PGA values along the fault zone occurred at stations within about 2 km of the town of Parkfield. The PGA in Parkfield is only 0.30 g, however, a fraction of the value at the surrounding stations. The reason for this difference is not yet clear.

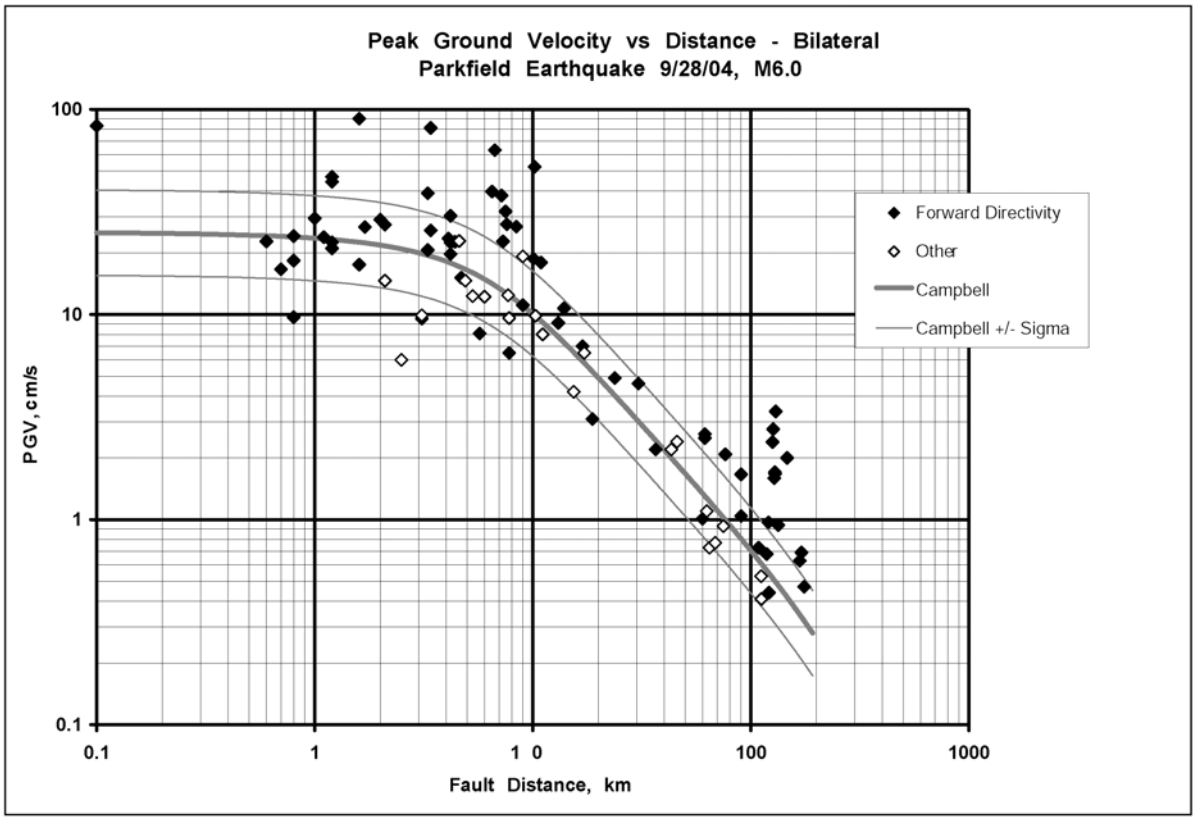

Figure 6. Peak velocity versus distance data separated according to forward directivity in the case of bilateral rupture propagation, similar to Figure 5.

Although several records have accelerations over 1 g, and one station, Fault Zone 16 is over 2.5 g, the largest well-recorded peak velocity is about 80 cm/sec (Fault Zone 15). This PGV is well below the largest values recorded in the 1994 M6.8 Northridge earthquake (150 cm/sec) and the values recorded in the 1999 M7.4 Taiwan Chi-Chi earthquake (300 cm/sec).

Some of the near-field records clearly reflect details of a complex rupture process. The displacement computed from the Fault Zone 15 record shows two pulses separated by about 3 seconds (Figure 7). This signal is so unusual that it might appear that there is a problem with a sensor or the processing. However the nearby stations Vineyard Canyon 1W and 2W also show this two-pulse signal, but with slightly different time separation. Thus, this shape is inferred to reflect radiation from the source, perhaps associated with local starting and stopping phases.

Several of the stations are ideally placed to record near-fault displacements, including the permanent offset. Unfortunately, two aspects work against the recovery of offsets from strong motion in this event. First, the event has relatively low slip (average slip of 15 cm, Langbein et al., 2005), and some of the actual visible slip at the fault did not occur until more than one hour after the event (i.e., the dynamic displacement signal occurred at the surface at the time of the rupture, but the static, permanent surface offset only occurred after near-surface soils yielded to the underlying motion to produce the

offset later). The second aspect is that the near-fault instruments are all film instruments, for which digitization limitations can easily lead to an uncertainty of several cm in the displacements at the period of a few seconds (e.g., Shakal et al., 2003). It may be possible to extract permanent displacements from some records, although even the dynamic displacement is only few cm at the stations near and over the rupture.

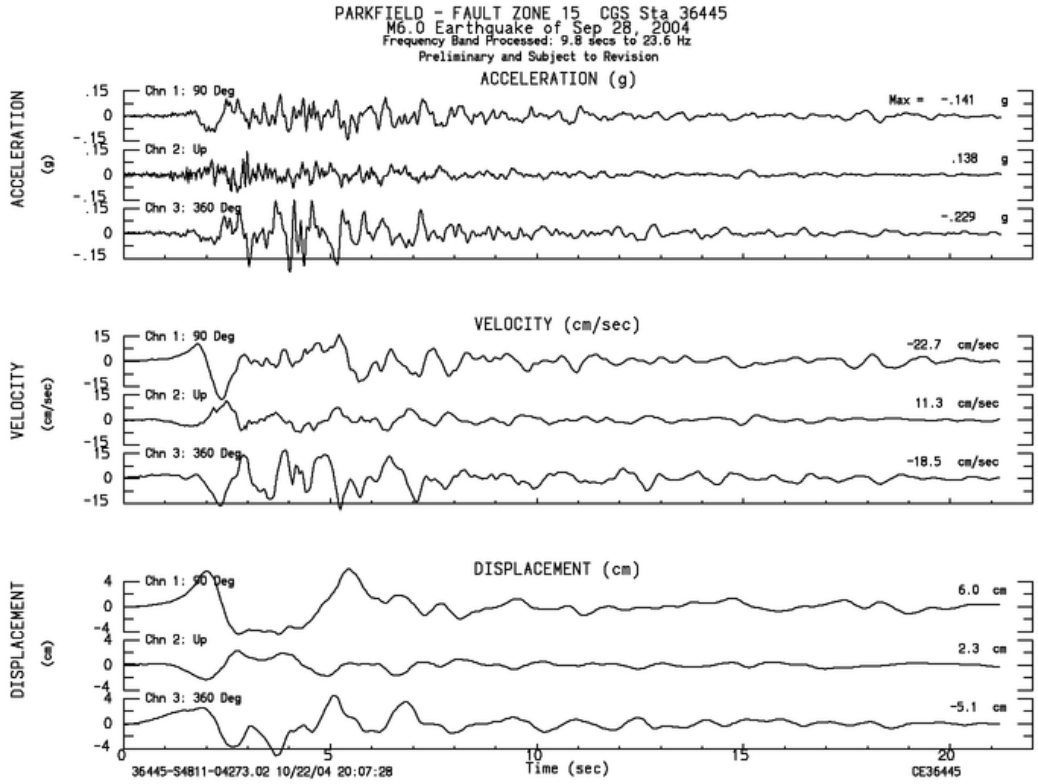

Figure 7. Acceleration, velocity and displacement at the Fault Zone 15 station, near Middle Mountain. The displacement shows two pulses separated by about 3 seconds, inferred to be associated with starting and stopping phases of rupture. Nearby stations (Vineyard Canyon 1W and 2W) also show these pulses.

Particle Motions in the Near-Fault Region

Even though the near-fault motion is very complex, there are clear fault-normal pulses at stations near the ends of the rupture. These are shown on a map on which the displacement particle motions are plotted at the station locations (Figure 8). The stations at the southern end of Cholame Valley have the greatest displacement, mostly normal to the fault. The greatest amplitude is at Fault Zone 1, about 12 cm, perpendicular to the

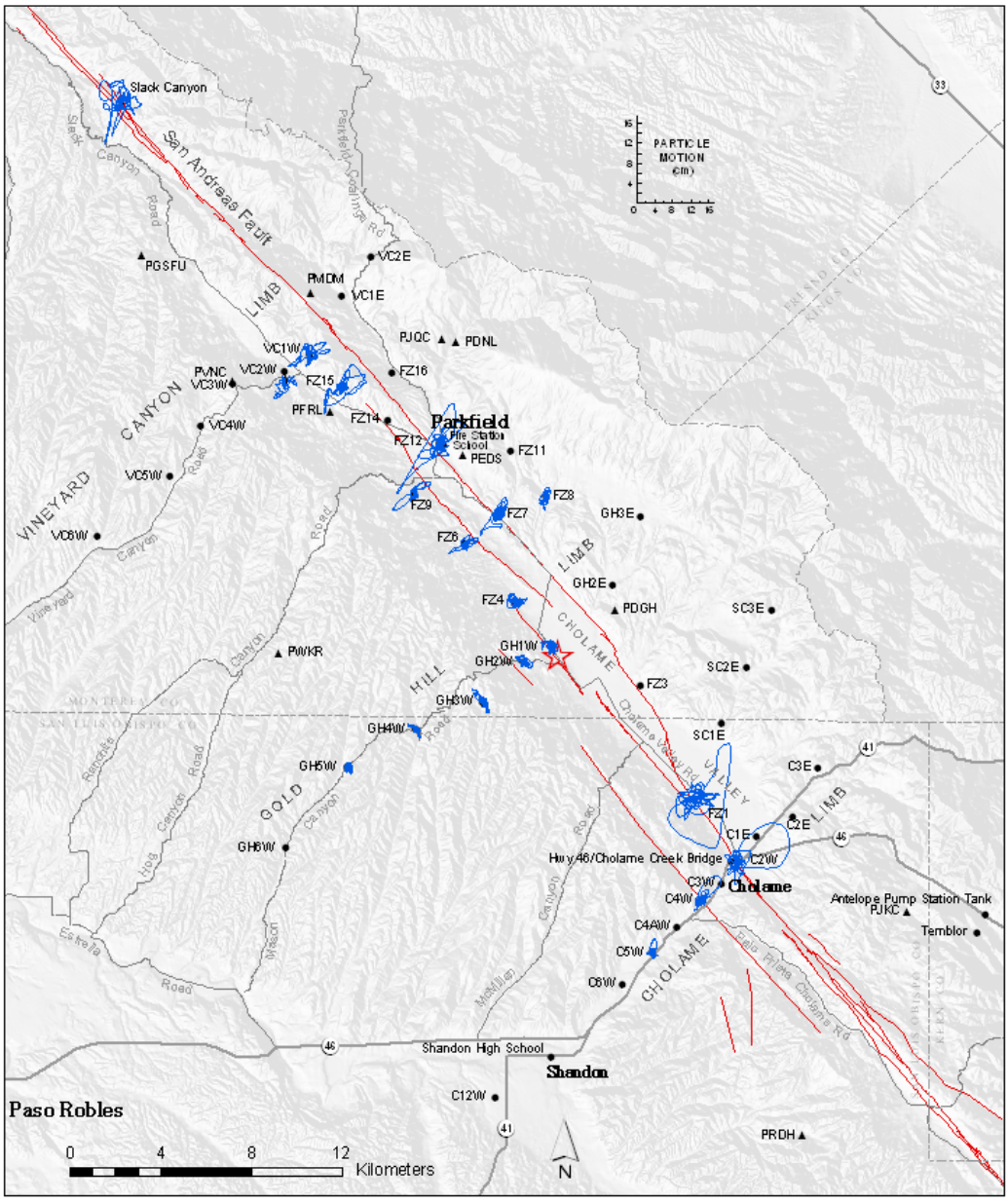

Figure 8. Horizontal displacement particle motions at stations in the near-fault region. The displacements obtained from integrating and processing the accelerograms are plotted at the corresponding locations of the stations. The fault-normal motions at stations near the ends of the fault are the largest amplitude displacements observed.

fault. Stations at the northern end of the fault also have significant fault-normal motions. The greatest is at Parkfield itself (Fault Zone12), where a displacement of ~10 cm occurs, almost exactly perpendicular to the fault. The motion at Fault Zone 16, not included in this figure, was almost perpendicular to the fault before the traces exceeded the instrument's recording capacity.

Two observations can be made for this set of near-fault measurements regarding the fault-normal motion. First, this motion is significant predominantly at the two ends of the fault. At intermediate stations in the central part of the fault, the fault-normal pulse is absent or small. Second, the amplitude of this pulse decays relatively rapidly away from the fault. The fault-normal pulse can be seen at stations of the Cholame limb, but it is smaller at 3W, and much smaller at 5W.

Ratios of Vertical to Horizontal Motion

The ratio of vertical to horizontal peak ground acceleration, usually called the V/H ratio, is an important parameter in some engineering applications. For the Parkfield earthquake data, the average V/H ratio is 0.49 (log normal, with +/- sigma variations from 0.33 to 0.72). An attempt was made to identify any differences in the V/H ratio with distance to the fault, especially for the near-fault region, and it was found that the

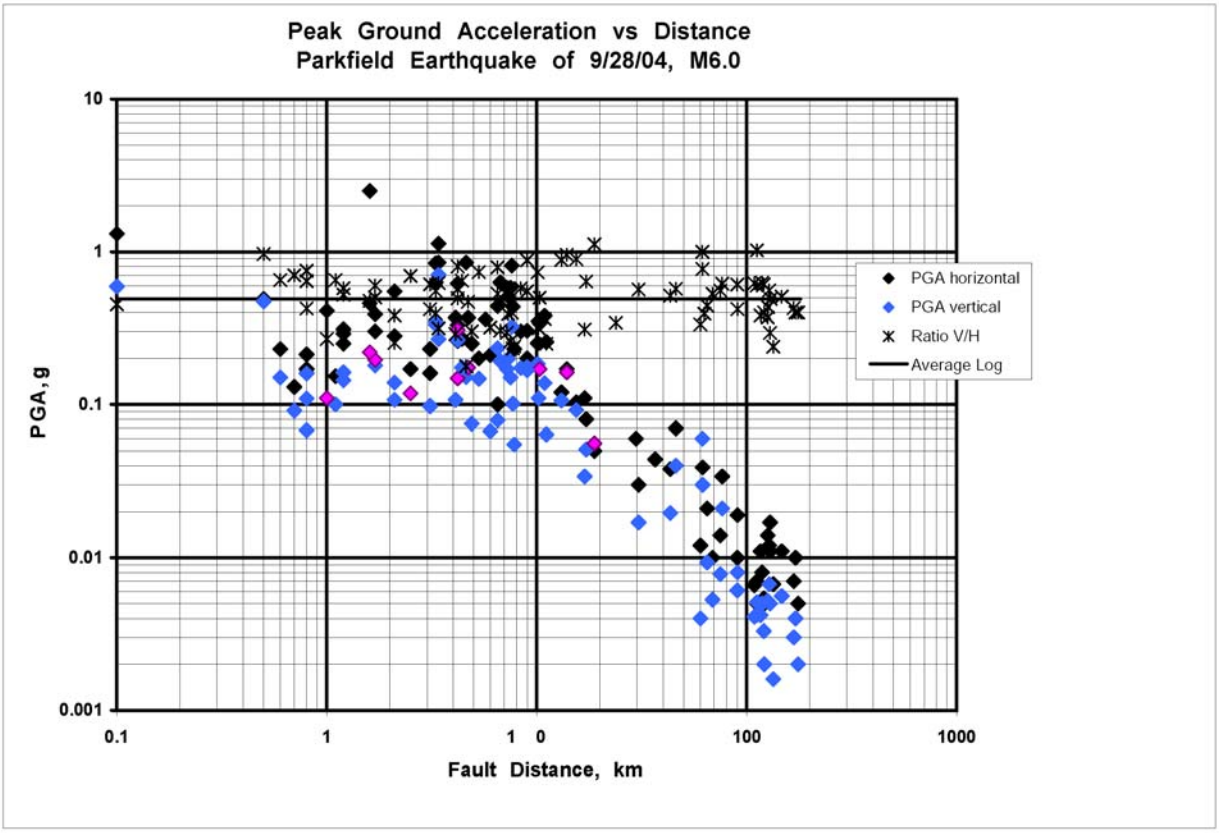

Figure 9. Comparison of the vertical and horizontal peak ground accelerations, and V/H ratios, for the Parkfield earthquake. The average V/H ratio for Parkfield is 0.49, similar to an overall ratio of 0.47 derived from 18 Californian earthquakes.

variations were insignificant. The investigation was extended to include strong motion data from 18 earthquakes of M > 5.5 (820 records). Based on this set of data Graizer and Shakal (2005) found that the V/H ratio is best described by log normal distribution, with an overall average ratio of about 0.47. The average ranges from 0.29 up to 0.69 for different earthquakes.

Response Spectra in the Near-Fault Region

The response spectra of four stations in the fault zone area are plotted in Figure 10. They show that several records have predominantly high frequency spectral accelerations, as expected. However, several records also have high motions at periods near 1 second, which are potentially more damaging to many structures. The motion in Parkfield, though it has low peak acceleration, has significant energy at longer periods.

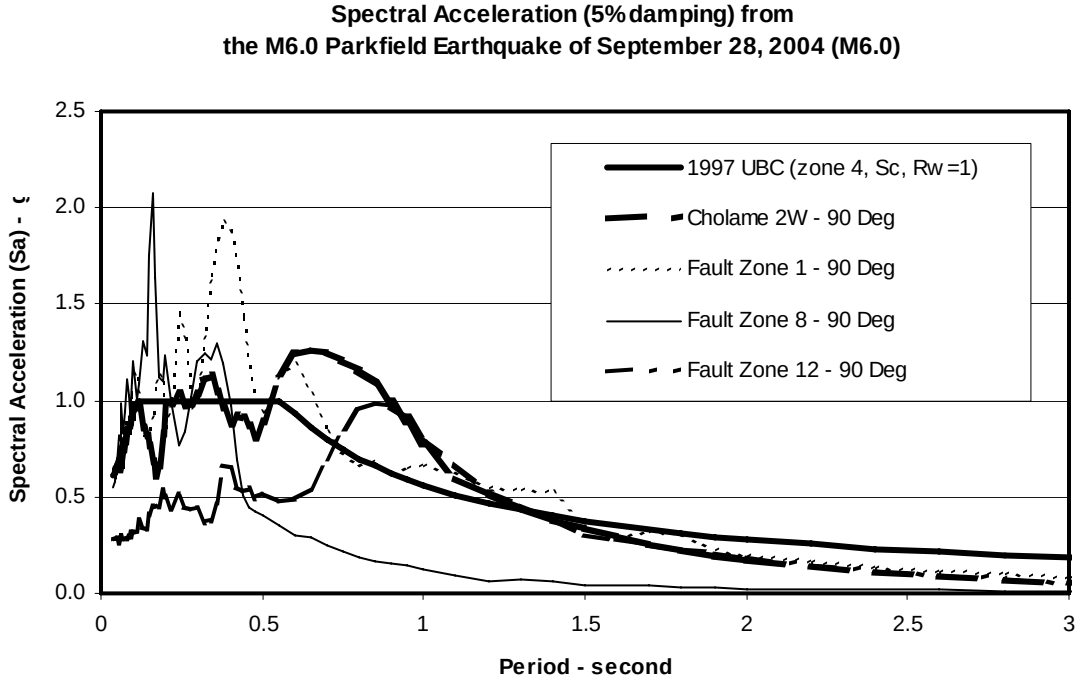

Figure 10. Comparison of acceleration response spectra at stations in the near-fault region. High frequency motion is seen at most stations, except Fault Zone 12. Stations near the ends of the rupture (Fault Zone 1, Cholame 2W, Fault Zone 12) have significant energy at periods near 1 second also.

Strong-Motion Records from Structures

Although there were not many structures affected by the Parkfield earthquake, significant records were obtained from a Caltrans bridge on Highway 46 and two buildings at Parkfield. Post-earthquake inspection indicated that these structures did not suffer any structural damage.

The Cholame Creek bridge on Highway 46 is located about 150m (500 ft) west of the San Andreas Fault and 90 m (290 ft) west of the ground response station Cholame

2W. The bridge (128.5' long 32.5' wide) was built in 1954 and widened to 43.5' in 1979. The bridge is a five-span concrete structure supported on concrete pile bents and abutments. The west abutment is monolithic with the pile foundation, while the east abutment is monolithic with the new foundation but is seated on the old foundation.

Acceleration records were obtained from the six sensors on the bridge (Figure 11). The records show that a sharp peak of about 1 g occurred at the east abutment in both the bridge longitudinal and transverse directions. Only 0.67g was recorded at the west abutment in the transverse direction, and 0.48g at the center of the bridge. This difference may be due to the fact that the east abutment is more flexible than the fully monolithic west abutment. Cracks were observed on the roadway asphalt near both abutments, but the structural integrity of the bridge was not compromised.

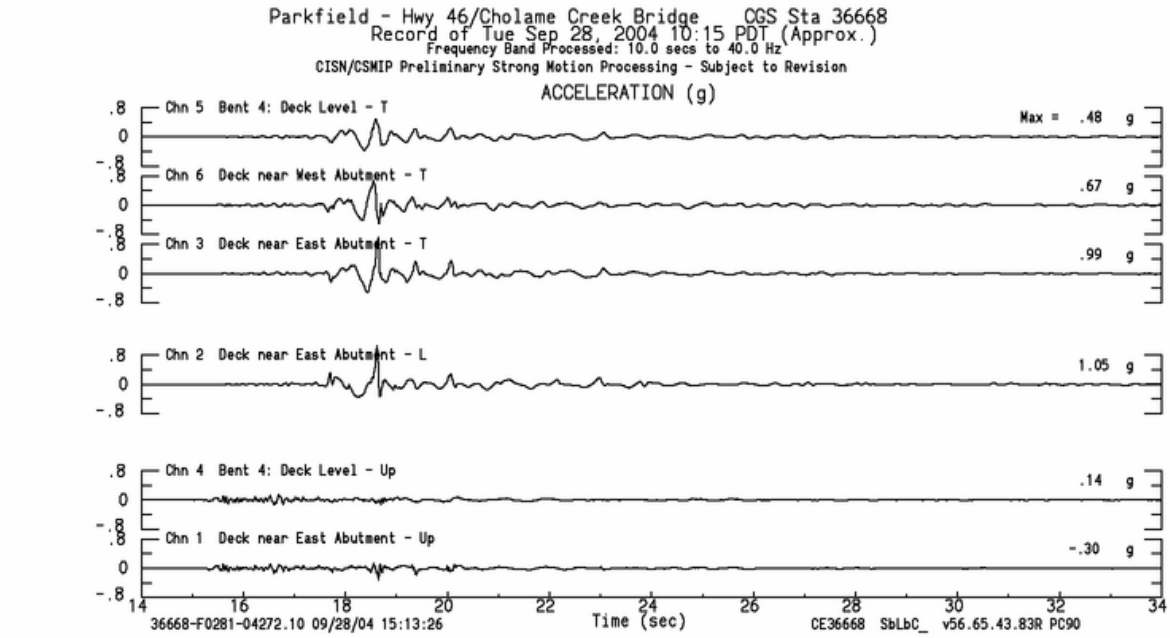

Figure 11. Acceleration records from the Cholame Creek Bridge at Highway 46. A large acceleration of about 1 g was recorded at the east abutment in both horizontal directions (channels 2 and 3). The motion recorded at the bridge is consistent with that at Station Cholame 2W, about 300 ft to the east. Despite this acceleration, the bridge did not suffer any structural damage.

The Parkfield Elementary School building is a 1-story wood frame structure built in 1949. The building has a plan dimension of 48 by 30 feet and a height of 13 feet. Accelerations records were obtained from the six sensors installed in the building (Figure 12). The maximum acceleration on the ground floor was 0.28 g in the N-S direction and 0.23g in the E-W direction, consistent with the motion recorded at the nearby ground response station Fault Zone 12, about 65 m (200 ft) from the school. The maximum acceleration recorded on the roof was 0.35g. Analyses of the displacements and response spectra of the records shows that the building period is about 0.2 second. With

this level of shaking, the building basically moved with the ground, with very little deformation.

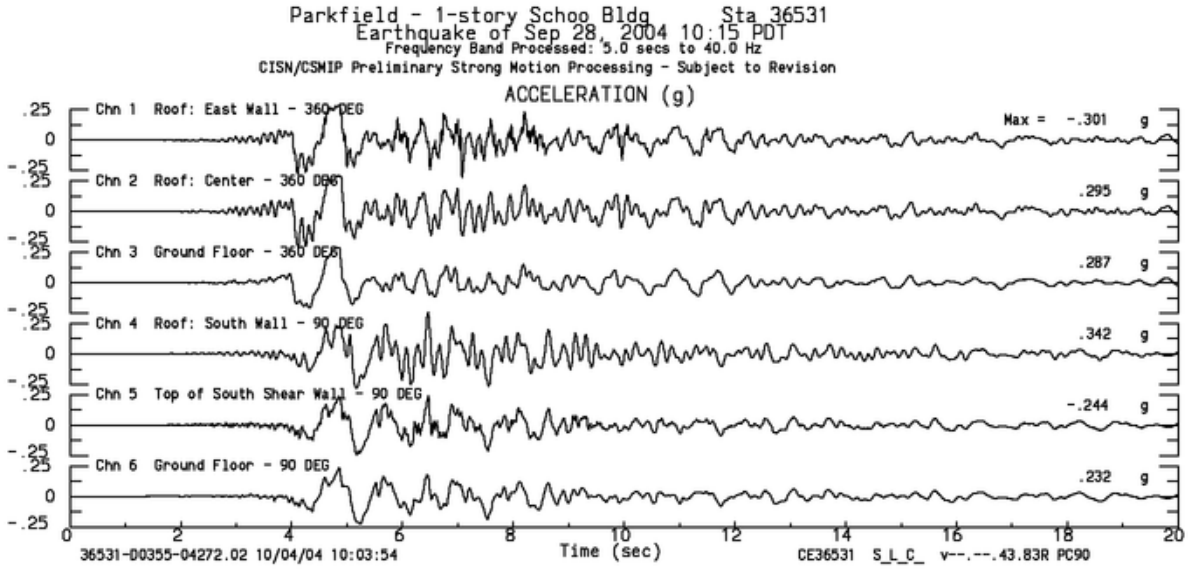

Figure 12. Acceleration records from the 1-story Parkfield Elementary School building. The recorded motions on the ground floor of the building are similar to those recorded at station Fault Zone 12, about 200 ft to the west. For this motion, the building moved with the ground, with very little deformation, and the building did not suffer any structural damage.

Turkey Flat Experiment

In anticipation of the Parkfield earthquake, the CGS established a test area in a sedimentary valley at Turkey Flat, east of Parkfield, California in the late 1980s (Real and Tucker, 1987). The test site was instrumented with a strong motion array by CSMIP, and CGS partnered with the IASPEI/IAEE Joint Working Group on Effects of Surface Geology on Seismic Motion, as well as members of the geotechnical community, to thoroughly characterize the geophysical properties of the site. The strong motion array consists of surface and downhole accelerometers, with surface instruments at the two valley edges, at one quarter of the valley width, and at the center of the small, shallow 24m (80 ft) stiff-soil sedimentary valley. The instruments at the valley center also include a downhole array, with instruments just below the rock interface and at mid-height in the sediments.

The Parkfield earthquake was well recorded throughout this array, providing the records necessary to conduct the long awaited blind prediction test. In this prediction experiment, acceleration time histories recorded on bedrock near one valley edge will be provided to participants, along with a “standard” model of the subsurface geotechnical properties at all recording sites. Participants will be asked to make predictions of the ground motions at the valley center and other recording locations for which, as part of a

long-term plan, records are not being made public until the predictions have been received and officially logged. A workshop at which predictions can be presented and comparisons made with the recorded motions is planned for late 2005. Details of the test area and the test procedure are available at http://www.quake.ca.gov/turkeyflat.htm.

Data Access

All of the data discussed here is available through the California Integrated Seismic Network's (CISN) Engineering Data Center (EDC), a joint effort of the CGS California Strong Motion Instrumentation Program and the USGS National Strong Motion Program. The files for all records are available at http://www.cisn-edc.org, having gone through digitization (if necessary), processing, and error checking. Both the processed data and the raw data are available and can be downloaded.

The GEOS recordings are available from the Internet at several locations as well as the CISN EDC. They are available from the Web site maintained by the National Strong-Motion Program in COSMOS format at http://nsmp.wr.usgs.gov/, linked to the COSMOS Virtual Data Center at http://www.cosmos-eq.org.

Summary

The Parkfield 2004 earthquake yielded the most extensive set of strong-motion data in the near source region of a magnitude 6 earthquake yet obtained. The spatial density of the measurements along the fault zone and in the linear arrays perpendicular to the fault provides an exceptional opportunity to develop improved models of the rupture process. The closely spaced measurements help infer the temporal and spatial distribution of the rupture process at much higher resolution than previously possible.

The peak acceleration data vary significantly along the rupture zone, from 0.13 g to over 2.5 g, with the largest values concentrated at the two ends. Particle motions at the near-fault stations are consistent with bilateral rupture. Fault-normal pulses similar to those observed in recent strike-slip earthquakes are apparent at several of the stations. The attenuation of peak ground acceleration with distance is more rapid than that indicated by some standard relationships. Evidence for directivity in the peak acceleration data is not strong, but it is clearer in the peak velocity data. Several stations very near, or over, the rupturing fault recorded relatively low accelerations. These recordings may provide a quantitative basis to understand observations of low near-fault shaking damage that has been reported in strike slip earthquakes.

Acknowledgements

Station siting permission from property owners in the Parkfield area made the instrument arrays possible. Installation the CGS stations was performed or overseen by Marvin Huston. Marvin, Tom Shipman and Ron Ayala performed most of the field data recovery; Bill Thompson maintained the stations carefully for the last 10 years, and Christopher Dietel maintained the USGS GEOS stations for years. Maintenance of

stations in remote areas like Parkfield, where neither power nor ready communication is available and access may be difficult, is a particularly difficult and tedious challenge; the success in recording data in this event depended on the diligent work of the individuals mentioned above. Pete Roffers generated the graphics that very effectively show the stations, geology and faults.

References

Abrahamson, N.A. and W.J. Silva (1997). Empirical response spectral attenuation relations for shallow crustal earthquakes, *Seismological Research Letters* **68**, 94-127.

Bakun, W.H. and T.V. McEvilly (1984). Recurrence models and Parkfield, California, earthquakes, *Journal Geophys. Research*, **89**, 3051-3058.

Boore, D.M., W.B. Joyner, and T.E. Fumal (1997). Equations for estimating horizontal response spectra and peak acceleration from western North American earthquakes: A summary of recent work, *Seismological Research Letters* **68**, 128-153.

Borcherdt, R.D. and M.J.S. Johnston (1988). A broadband, wide dynamic range, strong-motion network near Parkfield, California USA for measurement of acceleration and volumetric strain: *Proc. Ninth World Conference on Earthquake Engineering*, **VIII**, 125-130.

Borcherdt, R.D., J.B. Fletcher, E.G. Jensen, G.L. Maxwell, J.R. Van Schaack, R.E. Warrick, E. Cranswick, M.J.S. Johnston, and R. McClearn (1985). A general earthquake observation system (GEOS): *Bulletin of the Seismological Society of America* **75**, 1783-1825.

Borcherdt, R.D., M.J.S. Johnston, C. Dietel, G. Glassmoyer, G. Myren, and C. Stephens (2004). Acceleration and Volumetric Strain Generated by the Parkfield 2004 Earthquake on the GEOS Strong-Motion Array near Parkfield, CA, *US Geological Survey Open File Report* **2004-1376**, 75pp.

Campbell, K.W. (1997). Empirical near-source attenuation relationships for horizontal and vertical components of peak ground acceleration, peak ground velocity, and pseudo-absolute acceleration response spectra, *Seismological Research Letters* **68**, 154-179.

Cloud, W.K. and V. Perez (1967). Accelerograms – Parkfield Earthquakes, *Bulletin of the Seismological Society of America* **57**, 1179-1192.

Dibblee, T.W., Jr. (1973). Regional geologic map of San Andreas and related faults in Carrizo Plain, Temblor, Caliente, and La Panza ranges and vicinity, California, *U.S. Geological Survey Misc. Geologic Investigations Map* **1-757**, scale1:125,000.

Dickinson, W.R. (1966). Structural relations of San Andreas fault system, Cholame Valley and Castle Mountain Range, California: *Geological Society of America Bulletin*, **77**, 707-725.

Dreger, D. (2004). 09/28/2004 Preliminary slip model. *CISN website*: www.cisn.org/special/evt.04.09.28/finite.dreger.html

Graizer, V.G. and A.F. Shakal (2005). Attenuation of peak ground motion and V/H ratios for three recent California earthquakes (abs.), *Seismological Research Letters* **76**, 237.

Idriss, I.M. (1993). Procedures for selecting earthquake ground motions at rock sites, NIST Report GCR 93-625.

Jennings, C.W. (compiler) (1977). Geologic Map of California, Geologic Data Map Series No. 2, California Department of Conservation, California Geological Survey.

Langbein, J., R.D. Borcherdt, D. Dreger, J. Fletcher, J.L. Hardebeck, M. Hellweg, C. Ji, M. Johnston, J.R. Murray, R. Nadeau, M. Rymer and J. Treiman (2005). Preliminary report on the 28 September 2004, M 6.0 Parkfield, California earthquake, *Seismological Research Letters* **78**, 10-26.

Liu, P., S. Custodio and R. Archuleta (2005). Finite-fault model of the 2004 Mw6.0 Parkfield earthquake from inversion of strong-motion data (abs.), *Seismological Research Letters* **76**, 210.

McJunkin, R.D. and A. F. Shakal (1983) The Parkfield Strong-Motion Array, *California Geology* **36**, 27-34.

Real, C.R. and B.E. Tucker (1987). Ground Motion Site Effects Test Area at Turkey Flat, California: *EOS, Transactions American Geophysical Union* **68**, 1350.

Sadigh K., C.-Y. Chang, J.E. Egan, F. Makdisi and R.R. Youngs (1997). Attenuation relationships for shallow crustal earthquakes based on California Strong Motion Data, *Seismological Research Letters* **68**, 180-189.

Shakal, A.F. and R.D. McJunkin (1983). Preliminary summary of CDMG strong-motion records from the 2 May 1983 Coalinga, California, earthquake, Calif. Dept. Conservation, Office of Strong Motion Studies, OSMS **83-5.2**, 49p.

Shakal, A.F., M.J. Huang and V.M Graizer (2003). Strong motion data processing, p. 967-981 *in* Intl. Handbook on Earthquake and Engineering Seismology, W.H.K. Lee, H. Kanamori, P.C. Jennings and C. Kisslinger, eds., Academic Press.

Shakal, A.F., V. Graizer, M. Huang, R. Borcherdt, H. Haddadi, K. Lin, C. Stephens and P. Roffers (2005). Preliminary analysis of strong-motion recordings from the 28 September 2004 Parkfield, California earthquake, *Seismological Research Letters* **76**, 27-39.